https://africanjournalofbiomedicalresearch.com/index.php/AJBR
Afr. J. Biomed. Res. Vol. 28(2s) (February 2025); 712-731
Research Article

Exploring The Therapeutic Potential Of Benzimidazole-Diethylenediamine, Hexahydro-Pyrazine, 1,4-Diazacyclohexane Conjugates: A Synthetic Approach Towards The Development Of Antidiabetic And Antioxidant Agents

Stuti Verma[1*], Anup Kumar Sirbaiya[2], Priyanka Yadav[3]

[1*]Department of Pharmacy, Aryakul College of Pharmacy and Research, Sitapur, Uttar Pradesh, India
[2]Department of Pharmacy, KP Singh Memorial Institute of Pharmacy, Sitapur 261207
[3]Assistant professor faculty of pharmacy united University Jhalwa, Rawatpur, Prayagraj, Uttar Pradesh 211012

Abstract
A new 6-(4-substitue-piperazin-1-yl)-2-aryl-1*H*-benzimidazole derivatives were designed and expeditiously synthesized starting from 5-(4-phenylpiperazin-1-yl)-2- nitroaniline or 5-(4-ethylpiperazin-1-yl)-2-nitroaniline with different aldehydes. The piperazine ring was located at the C-6 of the successfully synthesized benzimidazole derivatives. Conventionally, this kind of reaction occurs with two steps: reduction and cyclization. This study's quick "one-pot" nitro reductive cyclization reaction employing sodium dithionite as a reagent made the synthetic technique efficient. The potential for both antioxidant and antidiabetic effects was investigated in all synthesized new substances. The newly synthesized compounds showed α-glucosidase inhibitory potential between IC_{50} = 0.85 ± 0.25 - 29.72 ± 0.17 μM and α-amylase inhibition potential between IC_{50} = 4.75 ± 0.24 - 40.24 ± 0.10 μM. Among the investigated compounds, 1f demonstrated the most substantial α-glucosidase and α-amylase inhibitory activities, with an IC_{50} value of 0.85 ± 0.25 μM, 4.75 ± 0.24 μM, respectively. According to the analysis of the kinetic experiments, these chemicals inhibit a competitive mechanism. Additionally, molecular docking experiments revealed the interaction profile of each drug when assessing their dock scores to obtain insight into how each chemical would bind to the α-glucosidase and α-amylase enzymes.

Keywords*:* Benzimidazole; Piperazine; One-pot; Synthesis; Antioxidant; α-Glucosidase; α- Amylase.

Received: 01/02/2025 *Accepted: 10/02/2025*

DOI: https://doi.org/10.53555/AJBR.v28i2S.6930

© 2025 The Author(s).
This article has been published under the terms of Creative Commons Attribution-Noncommercial 4.0 International License (CC BY-NC 4.0), which permits noncommercial unrestricted use, distribution, and reproduction in any medium provided that the following statement is provided. "This article has been published in the African Journal of Biomedical Research"

Introduction

Antioxidants can block DNA mutations, cancerous alterations, oxidative stress, and different types of cell harm in low quantities. (Ahmad et al., 2024)They can also prevent or postpone biomolecule oxidation (proteins, nucleic acids, lipids, and carbohydrates) [1]. By measuring a substance's ability to scavenge 2,2-diphenyl-1-picrylhydrazyl (DPPH) radicals, spectrophotometry is typically used to establish its antioxidant potential. The DPPH radical model is the most widely used method for fast evaluation of organic compounds' free radical scavenging ability.

Substantial evidence has accumulated and indicated key roles for reactive oxygen species (ROS) and other oxidants in causing numerous disorders and diseases.(Muheyuddeen, Rav Divya, et al., 2023) The evidence has brought the attention of scientists to an appreciation of antioxidants for prevention and treatment of diseases, and maintenance of human health [5]. Human body has an inherent antioxidative

mechanism and many of the biological functions such as the antimutagenic, anti-carcinogenic, and anti-aging responses originate from this property [6,7]. Antioxidants stabilize or deactivate free radicals, often before they attack targets in biological cells [8]. Recently interest in naturally occurring antioxidants has considerably increased for use in food, cosmetic and pharmaceutical products, because they possess multifacetedness in their multitude and magnitude of activity and provide enormous scope in correcting imbalance [9,10]. The role of free radical reactions in disease pathology is well established and is known to be involved in many acute and chronic disorders in human beings, such as diabetes, atherosclerosis, aging, immunosuppression and neurodegeneration [11]. An imbalance between ROS and the inherent antioxidant capacity of the body, directed the use of dietary and /or medicinal supplements particularly during the disease attack. Studies on herbal plants, vegetables, and fruits have indicated the presence of antioxidants such as phenolics, flavonoids, tannins, and proanthocyanidins. The antioxidant contents of medicinal plants may contribute to the protection they offer from disease. The ingestion of natural antioxidants has been inversely associated with morbidity and mortality from degenerative disorders [6]. Liver diseases remain a serious health problem. It is well known that free radicals cause cell damage through mechanisms of covalent binding and lipid peroxidation with subsequent tissue injury. Antioxidant agents of natural origin have attracted special interest because of their free radical scavenging abilities [12]. The use of medicinal plants with high level of antioxidant constituents has been proposed as an effective therapeutic approach for hepatic damages.

Reactive oxygen species (ROS)(Muheyuddeen et al., 2022; Muheyuddeen, Husain Rayini, et al., 2023), which also include hydroxyl radicals (OH), superoxide anion radicals, singlet oxygen ($^1O_2$), and hydrogen peroxide (H_2O_2), are highly reactive species. Each of these radicals can produce further ROS(Muheyuddeen et al., 2022) [2]. Numerous diseases, including cancer, atherosclerosis, diabetes, and ischemic heart disease, can be brought on by reactive oxygen species, which have various adverse effects. [3]. Additionally, ROS is linked to food quality decay, which results in toxicity, rancidity, and the loss of crucial biochemical components in physiologic metabolism. [4]. Therefore, creating efficient, risk-free antioxidant reagents to remove free radicals from the human body is critical. Certain benzimidazole compounds' antioxidant and radical-scavenging abilities have recently been studied [5,6].

Diabetes mellitus (DM) is among the top 10 reasons for premature death, accounting for over 1,000,000 deaths worldwide. Tough there are two broad categories of diabetes, type-1 diabetes mellitus (T1DM) and type-2 diabetes mellitus (T2DM) which is the most widespread type. T2DM is a public health challenge and has contributed to human morbidity and premature mortality. prevalence of T2DM is 462 million in 2017 with a worldwide incidence rate of 6059 cases per 100,000 people and is projected to increase to 7079 cases per 100,000 people by 2030. incidence of T1DM was 15 per 100,000 people and the prevalence was 9.5% (95% CI 0.07 to 0.12) in the world, which was statistically significant. Diabetes mellitus is a metabolic disorder linked to aberrant glucose concentration in the plasma and leads to insulin deficiency and/or impaired insulin activity. Some factors that affect insulin expression and action are body mass index (BMI), physical inactivity, heavy alcohol consumption, genetic and epigenetics, predisposition, and tobacco smoking. characteristic feature of T1DM is often associated with autoimmune destruction of the pancreatic ß-cell, causing total insulin deficiency. classic symptoms include weight loss, polyuria, polydipsia, polyphagia, and ketoacidosis. Pancreatic ß-cells are essential for maintaining a balance in blood glucose levels by synthesizing and secreting insulin. Prolonged hyperglycemia results in the apoptotic death of pancreatic ß-cells, thus reducing the pancreatic ß-cell volume and stimulating aberrant insulin release and glucose uptake. Hyperglycemia also stimulates the heightened generation of reactive species via NADPH oxidase activity, which potentiates proinfammatory biomarkers, such as IL-1β, IL-6, and TNF-α. Diabetes and its complications, like other diseases, have been linked to free radical generation, with glucose autoxidation being a major source of free radicals in chronic hyperglycemia. Although free radical production is necessary for normal cellular homeostasis and the body's response to pathogens, many diabetes complications are caused by excessive free radical generation and oxidative stress. oxidative stress and inflammation caused by persistent hyperglycemia are major contributors to these diabetes complications. PI3K is a kinase that is involved in regulating both the uptake and utilization of cellular glucose. Based on experimental findings, it is now clear that the release and regulation of insulin by pancreatic cells takes place via a PI3K/AKT mediated pathway9,10. In addition to stimulating pancreatic β-cell survival by inhibiting FoxO1, it is implicated in lipotoxicity in pancreatic β-cells. Many studies have shown that the overexpression and activation of PI3K/AKT in β-cells stimulate insulin secretion while the overexpression of inactive mutated forms of this kinase in β-cells and a subsequent reduction in PI3k/AKT activity leads to a lack of insulin secretion [10-12].

For treating diseases like cancer, HIV, obesity, hepatitis, diabetes, and hyperlipoproteinemia, the enzyme *α*-glucosidase is highly beneficial. Clinical applications of *α*-glucosidase inhibitors such as miglitol, voglibose, and acarbose include delaying the fast production of blood glucose. Therefore, *α*-glucosidase inhibitors lower glucose levels after meals in type-2 diabetic individuals [7]. But when used in long-term therapy, they have several undesirable side effects, including flatulence, abdominal pain, diarrhea, and other gastrointestinal

issues [8]. Therefore, a desirable and anticipated investigation is finding new *α*-glucosidase inhibitors with few negative effects. The benzimidazole derivatives exhibited *α*- glucosidase and antidiabetic properties [9–12]. Therefore, finding novel benzimidazole compounds to use as *α*-glucosidase inhibitors is crucial. In the digestive system, metalloenzyme *α*-amylase breaks down the *α*-1,4-glycosidic bond of starch to produce reducing sugars, including maltose, maltotriose, and amylodextrin [13]. The endo-amylase family member *α*-amylase needs calcium ions for structural stability, activity, and stability. Microorganisms, plants, and mammals all have amylases. As a result, *α*-amylases are employed in various industries, including brewing and starch processing, textile, pharmaceutical, fermentation, paper, food, and detergent industries. Human *α*-amylase is an oligosaccharide chain with a three-dimensional structure that allows it to attach to substrates. [14]. The biologically active heterocycles benzimidazoles and their derivatives are well known and have a wide range of medical applications, including antibacterial, anticancer, antifungal, antihelminthic, antiproliferative, antiviral, antihypertensive, anti-inflammatory, antitubercular, and antiprotozoal activity [15–20]. As a result, a quick, inexpensive, and effective synthetic method to produce benzimidazoles is required.

Creating and testing many novel piperazine-modified benzimidazole derivatives for potential biological activity would be interesting. Despite extensive research on the pharmacological effects of the piperazine-containing moiety, it is essential to develop new heterocyclic systems. Piperazine nucleus includes Cyclizine (antihistamine), Norfloxacin (chemotherapeutic antibacterial), Clozapine (antipsychotic), Trazodone (antidepressant), Vardenafil (urological), and Imatinib (anticancer) which are frequently used as medications (Fig. 1) [21]. As a result, when using chemical diversity for medicinal chemistry goals, the heterocyclic system is an attractive scaffold. Therefore, given the potential for pharmaceuticals, it is crucial to synthesize new piperazine derivatives using efficient and straightforward techniques.

In this study, we demonstrate the synthesis of benzimidazole structures from 4-chloro-2- nitroaniline, a chemical with a secondary amine group at the C-6 position. According to the literature, obtaining benzimidazoles with costly catalysts like Pt and Pd requires three steps. [22,23]. However, we produced the same kind of benzimidazole derivatives using a two-step procedure and benign circumstances in this investigation.

The biological characteristics of the synthetic substances were evaluated in terms of their antioxidant and inhibitory actions against α-glucosidase and α-amylase. Because these chemical compounds have the potential to do so, we proposed combining a piperazine and a benzimidazole ring to test if this increased or decreased their effectiveness.

Experimental section

Chemistry

Uncorrected melting points were measured on capillary tubes using Büchi oil-heated melting point equipment. The IR spectra were captured using the ATR (Attenuated Total Reflectance) technique on a Perkin Elmer Spectrum 100 FTIR Spectrometer. Using TMS as the internal standard, the ^{1}H and ^{13}C NMR spectra were captured using an Agilent Premium spectrometer at 400 and 100 MHz, respectively. Using a Triple Stage Quadrupole Mass Spectrometer from Thermo Scientific called the TSQ Quantum Access MAX, heated electrospray ionization mass spectroscopy (MS-MS) (H-ESI) was studied. A Carlo Erba 1106 CHN analyzer was used to perform elemental analyses. The reagent grade quality of all the chemicals, solvents, and reagents utilized were those purchased from commercial sources.

Synthesis of 5-(substituted)-2-nitroaniline

A mixture of K_2CO_3 (1.68 g, 0.012 mol) and *N*-ethylpiperazine (1.1 mL, 0.01 mol) or *N*-phehylpiperazine (1.6 mL, 0.01 mol) was added to 15 mL DMF in a round-bottomed flask. At room temperature, the mixture was stirred for 15 minutes. After that, 5-chloro-2- nitroaniline (1.72 g, 0.01 mol) was added and mixed for 24 hours at 120 ˚C.

The progress of the reaction was monitored by TLC, eluent MeOH–DCM, 1:9. After completion of the reaction, the mixture was added to ice water and filtered. The solid residue was washed from hexane and crystallized from ethanol to get pure compounds **1** and **2**.

5-(4-Ethylpiperazine-1-yl)-2-nitroaniline (1)

Yield: 2.28 g, (91%) mp: 125-127 ˚C [24]; IR (ATR) ν, cm^{-1}: 3525-3398 (NH_2), 3166 (Ar-CH), 2967 (aliph-CH), 1567-1314 (NO_2), 1177 (C-N).

5-(4-Phenylpiperazine-1-yl)-2-nitroaniline (2)

Yield: 1.64 g, (55%) mp: 195-197 ˚C [25]; IR (ATR) ν, cm^{-1}: 3480-3365 (NH_2), 3059 (Ar-CH), 2972 (aliph-CH), 1587, 1319 (NO_2), 1221(C-N).

General procedure for the synthesis of 2-(aryl)-6-(4-substitutedpiperazin-1-yl)-1H- benzimidazole

Compound **1** (0.25 g, 1 mmol) or compound **2** (0.30 g, 1 mmol) were combined with the corresponding aldehyde (1 mmol) in 20 mL of ethanol and placed in a flask with a flat bottom, and the mixture was kept at room temperature for 30 minutes. A solution of $Na_2S_2O_4$ (1.74 g, 10 mmol) in water (5 mL) was added dropwise to this mixture. Then, the mixture was refluxed with stirring for 24 hours to afford compounds **1a–f** and 48 hours for compounds **2a– f**. The mixture was added to cold water and filtered when the reaction was finished (monitored by TLC, eluent AcOEt-hexane, 3:1). The solid residue was crystallized from ethanol to get derivatives **1a-f** and from ethyl acetate to afford compounds **2a-f**.

6-(4-Ethylpiperazin-1-yl)-2-(4-methoxyphenyl)-1H-benzimidazole (1c)

Yield: 0.29 g, (86%), mp: 164-166 °C; IR (ATR) ν, cm^{-1}: 3048 (NH), 2959 (Ar-CH), 2882 (Aliphatic-CH), 1632 (C=N). ^{1}H NMR (400 MHz, DMSO-d_6) δ, ppm (*J*, Hz): 1.06 (t, *J*=8 Hz, 3H, CH_3), 2.50 (k, *J*=8 Hz, 2H, CH_2) 2.67 (bs, 4H, CH_2), 3.14 (bs, 4H, CH_2), 3.81 (s, 3H, CH_3), 6.88-8.05 (m, 7H, Ar-CH), 12.44 (s, H, NH). ^{13}C(APT)-NMR (100 MHz, DMSO- d_6) δ, ppm: 11.91, 50.04, 51.94, 52.67, 55.74 (CH_3), 56.48 (CH_2), 114.09, 114.73, 120.56, 123.47, 128.05, 132.24, 137.67, 139.68, 147.83, 151.03, 160.70 (Ar-C). Anal. Calcd for $C_{20}H_{24}N_4O$: C, 71.40; H, 7.19; N, 16.65. Found: C, 71.38; H, 7.18; N, 16.62. ESI-MS *m/z* (%): 337.11 $[M+H]^+$ (100).

6-(4-Ethylpiperazin-1-yl)-2-(4-methylphenyl)-1H-benzimidazole (1d)

Yield: 0.27 g, (84%), mp: 230-232 °C; IR (ATR) ν, cm^{-1}: 3095 (NH), 3039 (Ar-CH), 2951 (Aliphatic-CH), 1615 (C=N). ^{1}H NMR (400 MHz, DMSO-d_6) δ, ppm (*J*, Hz): 1.05 (t, *J*=8 Hz, 3H, CH_3), 2.35 (s, 3H, CH_3), 2.51 (k, *J*=8 Hz, 2H, CH_2) 2.70 (bs, 4H, CH_2), 3.17 (bs, 4H, CH_2), 6.61-8.32 (m, 7H, Ar-CH), 12.29 (s, H, NH). ^{13}C(APT)-NMR (100 MHz, DMSO- d_6) δ, ppm: 12.14, 20.01 (CH_3), 50.06, 51.83, 52.50, 56.24 (CH_2), 113.98, 121.02, 123.14, 128.46, 129.11, 130.91, 132.14, 136.56, 140.15, 147.94, 151.19 (Ar-C). Anal. Calcd for $C_{20}H_{24}N_4$: C, 74.97; H, 7.55; N, 17.48. Found: C, 74.93; H, 7.56; N, 17.50. ESI-MS *m/z* (%): 321.21 $[M+H]^+$ (100).

6-(4-Ethylpiperazin-1-yl)-2-(4-chlorophenyl)-1H-benzimidazole (1e)

Yield: 0.31 g, (94%), mp: 258-260 °C; IR (ATR) ν, cm^{-1}: 3134 (NH), 3037 (Ar-CH), 2950 (Aliphatic-CH), 1626 (C=N), 832 (C-Cl). ^{1}H NMR (400 MHz, DMSO-d_6) δ, ppm (*J*, Hz): 1.11 (t, *J*=8 Hz, 3H, CH_3), 2.42 (k, *J*=8 Hz, 2H, CH_2), 2.54 (bs, 4H, CH_2), 3.13 (bs, 4H, CH_2), 6.75-8.24 (m, 7H, Ar-CH), 12.54 (s, H, NH). ^{13}C(APT)-NMR (100 MHz, DMSO-d_6) δ, ppm: 12.84 (CH_3), 50.14, 51.98, 52.83, 56.17 (CH_2), 115.21, 118.82, 127.93, 129.13, 130.12, 132.15, 135.14, 137.21, 138.73, 148.69, 150.02 (Ar-C). Anal. Calcd for $C_{19}H_{21}ClN_4$: C, 66.95; H, 6.21; N, 16.44. Found: C, 66.93; H, 6.22; N, 16.41. ESI-MS *m/z* (%): 341.18 $[M+H]^+$ (100), 343.09 $[M+H+2]^+$ (38).

6-(4-Ethylpiperazin-1-yl)-2-(4-bromophenyl)-1H-benzimidazole (1f)

Yield: 0.33 g, (86%), mp: 156-158 °C; IR (ATR) ν, cm^{-1}: 3309 (NH), 3073 (Ar-CH), 2950 (Aliphatic-CH), 1624 (C=N), 687 (C-Br). ^{1}H NMR (400 MHz, DMSO-d_6) δ, ppm (*J*, Hz): 1.02 (t, *J*=8 Hz, 3H, CH_3), 2.37 (k, *J* =8 Hz, 2H, CH_2), 2.52 (bs, 4H, CH_2), 3.11 (bs, 4H, CH_2), 6.89-8.05 (m, 7H, Ar-CH), 12.66 (s, H, NH). ^{13}C(APT)-NMR (100 MHz, DMSO-d_6) δ, ppm: 12.36, (CH_3), 50.08, 52.05, 52.91, 56.48 (CH_2), 114.17, 119.51, 128.31, 130.13, 130.37, 132.31, 136.36, 138.32, 139.63, 148.71, 149.29 (Ar-C). Anal. Calcd for $C_{19}H_{21}BrN_4$: C, 59.23; H, 5.49; N, 14.54. Found: C, 59.20; H, 5.50; N, 14.53. ESI-MS *m/z* (%): 385.06 $[M+H]^+$ (100), 387.13 $[M+H+2]^+$ (100).

6-(4-Phenylpiperazin-1-yl)-2-phenyl-1H-benzimidazole (2a)

Yield: 0.30 g, (83%), mp: 240-242 °C; IR (ATR) ν, cm^{-1}: 3257 (NH), 3053 (Ar-CH), 2978 (aliph-CH), 1629 (C=N). ^{1}H NMR (400 MHz, DMSO-d_6) δ, ppm (*J*, Hz): 3.25 (bs, 4H, CH_2), 3.28 (bs, 4H, CH_2), 6.78 (t, J = 7.3 Hz, 1H, ArH), 6.98 (dd, J = 11.4, 8.6 Hz, 3H, ArH), 7.05 (d, J = 2.2 Hz, 1H, ArH), 7.21 (dd, J = 8.5, 7.0 Hz, 2H, ArH), 7.55 – 7.38 (m, 4H, ArH), 8.11 (d, J = 7.3 Hz, 2H, ArH), 12.59 (s, H, NH). ^{13}C(APT)-NMR (100 MHz, DMSO-d_6) δ, ppm: 48.97 (CH_2), 50.65, 108.96 (Ar-C), 114.82, 115.97, 116.05, 119.52, 126.52, 129.34, 129.43, 129.85, 130.83, 135.93, 148.27, 150.87, 151.43 (C=N). Anal. Calcd for $C_{23}H_{22}N_4$: C, 77.94; H, 6.26; N, 15.81. Found: C, 77.90; H, 6.26; N, 15.80. ESI-MS *m/z* (%): 355.28 $[M+H]^+$ (100).

6-(4-Phenylpiperazin-1-yl)-2-(4-hydroxyphenyl)-1H-benzimidazole (2b)

Yield: 0.28 g, (76%) mp: 242-244 °C; IR (ATR) ν, cm^{-1}: 3338 (OH), 3059 (NH), 3029 (Ar-CH), 2962 (Aliph-CH), 1629 (C=N). ^{1}H NMR (400 MHz, DMSO-d_6) δ, ppm (*J*, Hz): 3.21 (bs, 4H, CH_2), 3.28 (bs, 4H, CH_2), 6.78 (t, *J* = 7.3 Hz, 1H, ArH), 6.88 (d, *J* = 8.6 Hz, 2H, ArH), 6.91-7.09 (m, 4H, ArH), 7.16-7.26 (m, 2H, ArH), 7.40 (d, *J* = 8.7 Hz, 1H, ArH), 7.94 (d, *J* = 8.5 Hz, 2H, ArH), 9.88 (s, 1H, OH), 12.38 (s, 1H, NH). ^{13}C(APT)-NMR (100 MHz, DMSO-d_6) δ, ppm: 48.99 (CH_2), 50.80, 109.83 (Ar-C), 116.03, 116.06, 118.51, 119.49, 121.92, 128.22, 129.43, 131.85, 137.09, 147.86, 148.76, 151.44 (C=N), 159.21 (Ar-C). Anal. Calcd for $C_{23}H_{22}N_4O$: C, 74.57; H, 5.99; N, 15.12. Found: C, 74.54; H, 5.98; N, 15.10. ESI- MS *m/z* (%): 371.09 $[M+H]^+$ (100).

6-(4-Phenylpiperazin-1-yl)-2-(4-methoxyphenyl)-1H-benzimidazole (2c)

Yield: 0.32 g, (81%), mp: 268-270 °C; IR (ATR) ν, cm^{-1}: 3316 (NH), 3011 (Ar-CH), 2969 (Aliphatic-CH), 1627 (C=N). ^{1}H NMR (400 MHz, DMSO-d_6) δ, ppm (*J*, Hz): 3.22 (bs, 4H, CH_2), 3.27 (bs, 4H, CH_2), 3.81 (s, 3H, CH_3), 6.78 (t, J = 7.3 Hz, 1H, ArH), 6.88-7.02 (m, 4H, ArH), 7.04-7.09 (m, 2H, ArH), 7.18-7.25 (m, 2H, ArH), 7.45 (bs, 1H, ArH), 8.05 (d, J = 8.4 Hz, 2H, ArH), 12.48 (s, 1H, NH). ^{13}C(APT)-NMR (100 MHz, DMSO-d_6) δ, ppm: 48.98 (CH_2), 50.21, 55.74 (CH_3),

108.25 (Ar-C), 114.75, 116.04, 119.50, 120.38, 123.38, 124.23, 128.06, 129.43, 131.74, 132.85, 146.05, 148.10, 151.44 (C=N), 160.73 (Ar-C). Anal. Calcd for $C_{24}H_{24}N_4O$: C, 74.97; H, 6.29; N, 14.57. Found: C, 74.94; H, 6.30; N, 14.55. ESI-MS *m/z* (%): 385.21 $[M+H]^+$ (100).

6-(4-Phenylpiperazin-1-yl)-2-(4-methylphenyl)-1H-benzimidazole (2d)

Yield: 0.32 g, (84%) mp: 269-271 °C; IR (ATR) ν, cm^{-1}: 3302 (NH), 3069 (Ar-CH), 2958 (Aliph-CH), 1627 (C=N). ^{1}H NMR (400 MHz, DMSO-d_6) δ, ppm (*J*, Hz): 2.34 (s, 3H, CH_3), 3.22 (bs, 4H, CH_2), 3.28 (bs, 4H, CH_2), 6.78 (t, J = 7.3 Hz, 1H, ArH), 6.93-7.00 (m, 3H, ArH), 7.00-7.08 (m, 1H, ArH), 7.16-7.26 (m, 2H, ArH), 7.31 (d, J = 7.8 Hz, 2H, ArH), 7.44 (d, J = 8.7 Hz, 1H, ArH), 8.00 (d, J = 8.0 Hz, 2H, ArH), 12.47 (s, 1H, NH). ^{13}C(APT)-NMR (100 MHz, DMSO-d_6) δ, ppm: 21.40 (CH_3), 48.97 (CH_2), 50.69, 108.08 (Ar-C), 114.63, 116.04, 118.03, 119.50, 126.49, 128.13, 129.42, 129.90, 133.15, 136.14, 139.51, 148.15, 151.07, 151.43 (C=N). Found: C, 78.18; H, 6.56; N, 15.20. ESI-MS *m/z* (%): 369.10 $[M+H]^+$ (100).

6-(4-Phenylpiperazin-1-yl)-2-(4-chlorophenyl)-1H-benzimidazole (2e)

Yield: 0.30g, (77%) mp: 259-261 °C; IR (ATR) ν, cm^{-1}: 3246 (NH), 3048 (Ar-CH), 2964 (Aliph-CH), 1631 (C=N), 831 (C-CI). ^{1}H NMR (400 MHz, DMSO-d_6) δ, ppm (*J*, Hz): 3.23 (bs, 4H, CH_2), 3.27 (bs, 4H, CH_2), 6.79 (t, J = 7.3 Hz, 1H, ArH), 6.95-7.07 (m, 4H, ArH), 7.22 (td, J = 8.3, 7.4, 2.2 Hz, 2H, ArH), 7.48 (d, J = 8.8 Hz, 1H, ArH), 7.58 (dd, J = 8.7, 2.3 Hz, 2H, ArH), 8.15 – 8.12 (m, 2H, ArH), 12.64 (s, 1H, NH). ^{13}C(APT)-NMR (100 MHz, DMSO-d_6) δ, ppm: 48.95 (CH_2), 50.56, 109.60 (Ar-C), 115.00, 116.05, 119.53, 128.20, 129.43, 129.45, 129.74, 134.43, 137.07, 148.41, 148.78, 149.79, 151.41 (C=N). Anal. Calcd for $C_{23}H_{21}ClN_4$: C, 71.03; H, 5.44; N, 14.41. Found: C, 71.00; H, 5.45; N, 14.43. ESI-MS *m/z* (%): 389.25 $[M+H]^+$ (100), 391.14 $[M+H+2]^+$ (40).

6-(4-Phenylpiperazin-1-yl)-2-(4-bromophenyl)-1H-benzimidazole (2f)

Yield: 0.39 g, (91%), mp: 257-259 °C; IR (ATR) ν, cm^{-1}: 3261 (NH), 3048 (Ar-CH), 2971 (Aliphatic-CH), 1630 (C=N), 686 (C-Br). ^{1}H NMR (400 MHz, DMSO-d_6) δ, ppm (*J*, Hz): 3.18 (bs, 4H, CH_2), 3.25 (bs, 4H, CH_2), 6.68 (t, J = 7.3 Hz, 1H, ArH), 6.90-7.05 (m, 4H, ArH), 7.18 (td, J = 7.4 Hz, 2H, ArH), 7.31 (d, J = 8.8 Hz, 1H, ArH), 7.61-7.82 (m, 4H, ArH), 12.55 (s, 1H, NH). ^{13}C(APT)-NMR (100 MHz, DMSO-d_6) δ, ppm: 49.04, 51.28 (CH_2), 108.10, 115.12, 116.22, 118.15, 126.41, 127.78, 128.40, 128.92, 130.37, 135.14, 147.15, 148.79, 149.79, 152.14 (C=N). Anal.Calcd for $C_{23}H_{21}BrN_4$: C, 63.75; H, 4.88; N, 12.93. Found: C, 63.71; H, 4.89; N, 12.92. ESI-MS *m/z* (%): 432.21 $[M+H]^+$ (100), 434.18 $[M+H+2]^+$ (100).

Biological assay

Antioxidant Activity Methods

Using a variety of in vitro antioxidant assays, such as the DPPH (1,1-diphenyl-2- picrylhydrazyl), Cupric Reducing Antioxidant Capacity (CUPRAC) assays, and the Ferric Reducing Antioxidant Power (FRAP) assay, the antioxidant activities and radical scavenging properties of the synthesized compounds were clarified.

Cupric Reducing Antioxidant Capacity (CUPRAC) Assay

The literature was used to estimate the antioxidant capacity of the synthesized compounds to reduce cupric acid. [26,27]. The standard curve for Trolox® (Sigma Chemical Co., USA) was linear between 8 mg/mL and 0.03125 mg/mL (r^2=0.9987) when evaluated under the same circumstances as a standard antioxidant chemical. Values for CUPRAC were given as the mM Trolox equivalent of 1 mg of synthetic substance.

Ferric Reducing Antioxidant Power (FRAP) Assay

The total antioxidant capacity was calculated using the Ferric Reducing Antioxidant Power (FRAP) test. It used 25 ml of acetate buffer (300 mM, pH 3.6), 2.5 ml of a 10 mM TPTZ solution in 40 mM HCl, and 2.5 ml of a 20 mM $FeCl_3.6H_2O$ solution to make the FRAP reagent. [26–28]. A reference curve was built using six concentrations of FeSO4.7H2O as a positive control. (15.63–31.25–62.5–125–250–500–1000μM, r^2=0.999).

The $FeSO_4.7H_2O$ concentration from the graph corresponding to the absorbance seen with the sample was used to determine the FRAP values, represented as mM $FeSO_4.7H_2O$ equivalent per milligram of the compound.

DPPH−Free radical scavenging assay

The 1,1-diphenyl-2-picrylhydrazyl (DPPH) radical has been employed extensively as the model system to examine the scavenging abilities of many synthetic and natural chemicals. The synthesized compounds' ability to scavenge DPPH radicals was evaluated using a technique described in the literature [26,27,29]. Ascorbic acid was used as a reference for assessing the amount of radical scavenging activity, and all results are presented as SC_{50} (μg compound per mL), which is the sample concentration required to scavenge 50% of the DPPH radical. Daily new preparations of the DPPH radical stock solution were made. In the DPPH approach, butylated hydroxytoluene (BHT) was utilized as a positive radical scavenger molecule. Three different times were used to make each judgment.

α-Glucosidase inhibition assay

The spectrophotometric analysis assessed the inhibitory test for α-glucosidase from

Saccharomyces cerevisiae [30,31].

The formula used to determine the proportion of α-glucosidase inhibition was:

α — *glucosidase inhibition* (%) = [(*Acontrol* — *Asample*) / *Acontrol*] x100

where A_{sample} is the activity of the enzyme with the compound/standard at various doses, and $A_{control}$ is the activity of the enzyme without the compound/standard. The IC_{50} was established as the inhibitor concentration to block 50% of the enzyme activity under the test conditions. The substrate 4-pNPG was used to measure the enzyme's activity in the buffer (pH 6.8). A test tube of 5 µL of 20 U/mL α-glucosidase enzyme and increasing amounts of 4-pNPG (0.20-2.4 mg/mL) were added. The mixture was then incubated at 25 °C for 14 min. At 405 nm, the absorbance value was determined. According to the Lineweaver-Burke graph, the collected data was plotted as 1/activity (1/V) versus 1/substrate concentration (1/[S]) [32].

To ascertain the kind of α-glucosidase inhibition, the more active compounds (**1c, 1d, 1e, 1f, 2d, 2e, and 2f**) compared to standard and acarbose were further investigated. A buffer (pH 6.8) containing enzyme solution (20 U/mL), with **1c, 1d, 1e, 1f, 2d, 2e, 2f,** and acarbose or without inhibitor solutions, had substrate concentrations of 0.20, 0.40, 0.80, 1.6, and 2.4 mg/mL in the reaction medium. After obtaining the Lineweaver-Burk graphs, inhibition patterns were assessed.

α-Amylase inhibition assay

According to a previously published procedure, α-amylase activity was inhibited. [33,34]. The formula used to determine the proportion of alpha–amylase inhibition was:

α — *amylase inhibition* (%) = [(*Acontrol* — *Asample*) / *Acontrol*] x100

where A_{sample} is the activity of the enzyme with the compound/standard at various doses, and $A_{control}$ is the activity of the enzyme without the compound/standard. The IC_{50} was established as the inhibitor concentration to block 50% of the enzyme activity under the test conditions. Increasing amounts of starch solution (0.30-1.2 mg/mL) were used as substrates to measure the enzyme activity in a 0.02 M sodium phosphate buffer (pH 6.9). According to what was stated in the activity section above, the absorbance was measured at 540 nm. According to the Lineweaver-Burk graph, the collected data was plotted as 1/activity (1/V) versus 1/substrate concentration (1/[S]) [32].

To ascertain the kind of alpha-amylase inhibition, more research was conducted on the more active compounds (**1d, 1e, 1f, 2e, and 2f**) than standard acarbose. The enzyme solution in the buffer (pH 6.9), with (**1d, 1e, 1f, 2e,** and acarbose) or without inhibitor solutions, had substrate concentrations of 0.30, 0.40, 0.60, 0.80, and 1.2 mg/mL in the reaction medium. K_m and V_{max} values were computed, Lineweaver-Burke graphs were constructed, and inhibition patterns were assessed.

Molecular docking methodology

MOE (2016) software was used for a molecular docking investigation [35]. From the protein databank database (PDB), the 3D structure of α-amylase with PDB ID (3BAJ) was extracted [35] due to the non-availability of the crystal structure of α-glucosidase previously modeled structure by our group was used for docking study [30]. Before the energy minimization, all of the water molecules were eliminated. With MMFF94s force field, energy reduction was performed up to 0.05 gradients. The substrate-binding site of α-amylase was designated for molecular docking, and the 3D structural coordinates of all synthesized Benzimidazole derivatives were created and placed in a new MOE database. All ligand atoms were set to flexibility during docking to produce the low-energy ligand-protein combination. The GBVI/WSA dG score system was applied to rank the compounds. Finally, Pymol v.1.7 was employed to analyze the interactions of the ligand-protein complex [36].

Result and discussion

Chemistry

In recent years, various synthetic techniques have been created to introduce novel reagents with different heterocyclic systems to produce benzimidazoles. The piperazine cycle is typically found in benzimidazoles' N-1 or C-2 position in the literature [37–41]. However, getting this heterocyclic in the benzimidazole's C-6 position is challenging. 4-Chloro-2- nitroaniline is a well-known starting material for the nucleophilic replacement of piperazine with a chloro group.

The following step, which required highly oxidizing or acidic conditions, was the nitro group's reduction to an amine *via* hydrogenation [22,23] or reduction process [42,43]. This approach has several disadvantages, including a lengthy reaction path, intermediate isolation, expensive reagents, severe reaction conditions, time-consuming, low yield, and workup procedures. As a result, "one pot" reductive cyclization, advantageous to the stepwise cyclization technique, is cheap, practical, simple, and high-yielding compared to this stepwise method.

The reaction of 4-chloro-2-nitroaniline with *N*-ethylpiperazine and *N*-phenylpiperazine to yield 5-(4-ethylpiperazin-1-yl)-2-nitroaniline (**1**) and 5-(4-phenylpiperazin-1-yl)-2- nitroaniline (**2**) respectively served as the beginning of the synthetic sequence. [24,25].

By utilizing sodium dithionite reagent and different substituted aromatic aldehydes in a "one-pot" nitro reductive cyclization reaction with 5-(4-ethylpiperazin-1-yl)-2-nitroaniline **(1)** or 5-(4-phenylpiperazin-1-yl)-2-nitroaniline **(2)** under reflux conditions, the 2-(aryl)-6-(4- substitutepiperazin-1-yl)-1*H*-benzimidazole derivatives (**1a–f** or **2a-f**) were obtained (Scheme 1). Compared to traditional stepwise cyclization techniques, this "one pot" reductive synthesis of 1a-f and 2a-f produced a high purity with fair yield in a relatively short time.

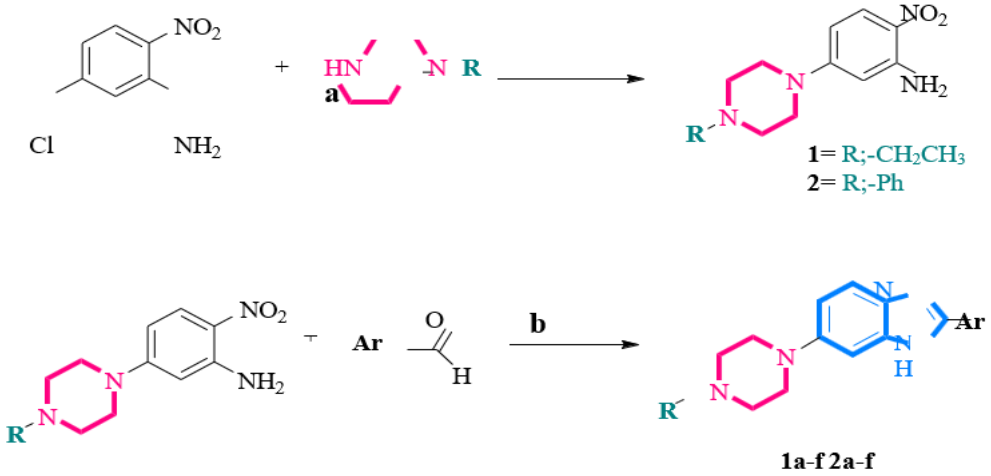

Scheme 1. Synthetic route to produce benzimidazole derivatives: *Reagents and conditions:*

(a) K_2CO_3, DMF, 120 ˚C, 24 h; **(b)** $Na_2S_2O_4$, EtOH, reflux 24 h

The possible mechanism for 2-(aryl)-6-(4-substitutepiperazin-1-yl)-1*H*-benzimidazole synthesis is provided in Scheme 2. After condensation with 4-substituted 2-nitroaniline, the aryl aldehyde undergoes an oxidation-reduction reaction to produce the corresponding imine. (**Scheme 2**). The nitro group is then reduced by all four electrons, making aniline derivatives; this results in *in situ* cyclization to create benzimidazoline [44]. Sulfur dioxide is produced on-site when sodium dithionite breaks down in water with atmospheric oxygen. As shown in Scheme 2, the resulting sulfur dioxide can oxidize the intermediate benzimidazoline to benzimidazole [45].

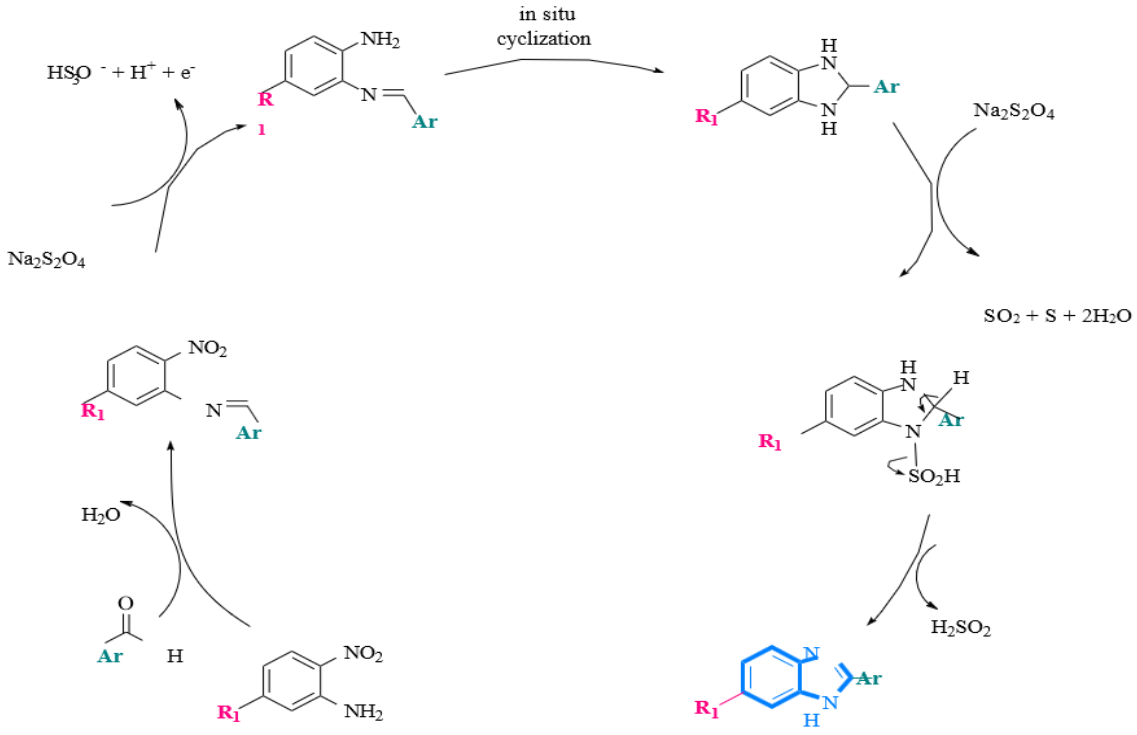

Scheme 2. The production of benzimidazoles: Potential processes

The compounds' structures were verified using FT-IR, 1H, ^{13}C-NMR spectroscopy, mass spectrometry (H-ESI), and elemental analysis. The biological activities of each synthesized substance were examined.

In vitro α-Glucosidase and α-Amylase Inhibitory Activities

The ability of the synthesized compounds to inhibit *α*-glucosidase and *α*-amylase was examined. All substances with inhibitory activity's IC_{50} values for -glucosidase were included in Table 1, and with an IC_{50} value of 0.85±0.04 µM, **1f**, the tested drug, demonstrated the most notable -glucosidase inhibition. (Table 1). The compounds that are more potent in inhibiting *α*-glucosidase than acarbose are given below in order of increasing potency for *α*-glucosidase inhibition: in order, **1f > 1e > 1d > 2f > 2e > 1c > 2d >** Acarbose **(**Table 1). Certain substances can significantly inhibit the α-glucosidase enzyme.

All synthesized compounds were able to inhibit *α*-amylase with an IC_{50} value in the range of IC_{50} = 4.75 ± 0.24 – 40.24 ± 0.10 *μ*M. The compounds **1f, 2f, 1e, 2e,** and **1d** were the most effective at inhibiting *α*-amylase, while compounds **1c, 2c,** and **2d** had a moderate activity level. However, **1f** was the most active derivative with an IC_{50} value of 4.75 ± 0.24. (**Table-1**).

Table 1. Effects of the synthetic compounds on in vitro *α*-amylase and *α*-glucosidase inhibition.

Compound No.	Ar	*α*-Amylase Inhibition	*α*-Glucosidase Inhibition
		IC_{50} ± SEM[a] (*μ*M)	IC_{50} ± SEM[a] (*μ*M)
Intermediate 1	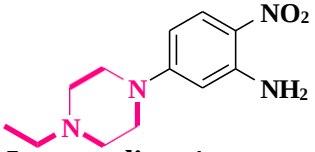	35.42 ± 0.25	33.45b ± 0.24
1a	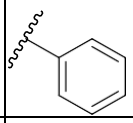	28.75 ± 0.14	22.68 ± 0.190
1b	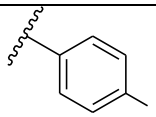	20.50 ± 0.13	15.43 ± 0.24
1c	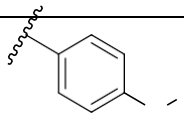	16.28 ± 0.09	10.24 ± 0.19
1d	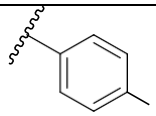	10.90 ± 0.12	4.16 ± 0.41
1e	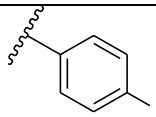	8.66 ± 0.21	2.74 ± 0.33
1f	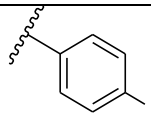	4.75±0.24	0.85±0.25
Intermediate 2	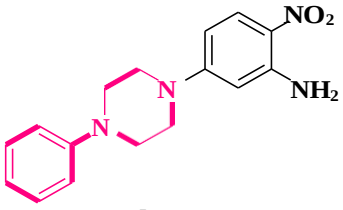	40.24 ± 0.10	29.72 ± 0.17
2a	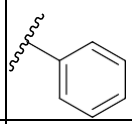	30.45 ± 0.27	25.88 ± 0.23
2b	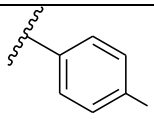	24.60 ± 0.19	20.56 ± 0.31

2c	**O** **CH_3** 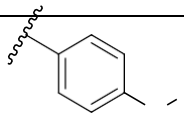	18.75 ± 0.15	16.95 ± 0.15
2d	**CH_3** 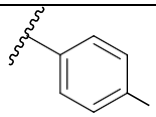	15.00 ± 0.33	11.70 ± 0.20
2e	**Cl** 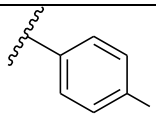	10.30 ± 0.27	9.82 ± 0.24
2f	**Br** 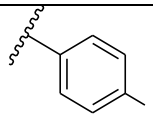	7.84 ± 0.17	5.60 ± 0.33
Standard[b] = Acarbose		14.70 ± 0.11	14.70 0.11

Structure-activity relationship (SAR)

The structure-activity relationship (SAR) of synthesized **1a-f** and **2a-f** was established based on different groups on the piperazine ring and differently substituted groups on the phenyl ring at the *para* position. Among the two intermediates, intermediate **I** was observed to be more active for *α*-amylase inhibition, and intermediate **II** was more active for *α*- glucosidase inhibition but not more than the standard acarbose. Moreover, within series **1** and **2**, generally, compounds **1a-f** exhibited more inhibitory potential than compounds **2a-f**. We concluded that the nonplanar position of the group results in increased activity.

Among all compounds, the **f** and **e** series, having bromo and chloro groups on the phenyl ring, exhibited better inhibitory results against both enzymes (Figure 2). It might result from the bromo and chloro groups' potent interaction with the active molecular location. In comparison to the standard, compound **1f** with a bromo group replaced inhibited the enzyme α-glucosidase with a potency that was seventeen times higher (IC_{50} = 0.85 ± 0.25 µM) and the enzyme α-amylase with a potency that was three times higher IC_{50} = 4.75 ± 0.24 µM). The presence of the bromine atom in compound **1f** makes it a more effective α-glucosidase inhibitor because it may be involved in strong hydrogen bonding interactions within the enzyme's pocket. The second-most active structure, chloro-substituted compound **1e**, showed two times higher inhibition of α-amylase (IC_{50} = 8.66 ± 0.21 µM) and five times more inhibition of α-glucosidase (IC_{50} = 2.74 ± 0.33 µM). Replacing the *para*-halo substituent with a methyl group for compound **1d** resulted in a decrease in activity. We concluded that enhanced activity results from intramolecular hydrogen bonding; however, the activity mostly affects the substituted nonplanar group (series 2).

The compounds **1b, 2c, 2b, 1a,** and **2a** exhibited less activity than standard acarbose (14.70 ± 0.11 µM). Compounds **1b, 2c,** and **2b** have electron donor groups such as -OH and - OCH_3, resulting in less activity. On the other hand, unsubstituted compounds **1a** (IC_{50} = 22.68
± 0.19 µM) and **2a** (IC_{50} = 25.88 ± 0.23µM) showed the least activity among all compounds
except intermediates **1** and **2**. It is concluded that the substitute group positively affected the activity with intramolecular interaction.

To identify the type of enzyme inhibition exhibited by the substances **1f, 1e, 1d, 2f, 2e, 1c, 2d,** and acarbose kinetic studies were carried out, Lineweaver-Burk plots were used to examine their α-glucosidase activity using information from enzyme assays with various doses of 4-pNPG in the absence or presence of each inhibitor. (Figures 3a-b, Table 2). The *K*m value increased while the V_{max} value (180.68 mM/min) stayed constant in the presence of **1c, 1d, 1e, and 1f**. From this perspective, the Lineweaver-Burk plots analysis showed that these structures' inhibition mode was competitive (Figure 3a).

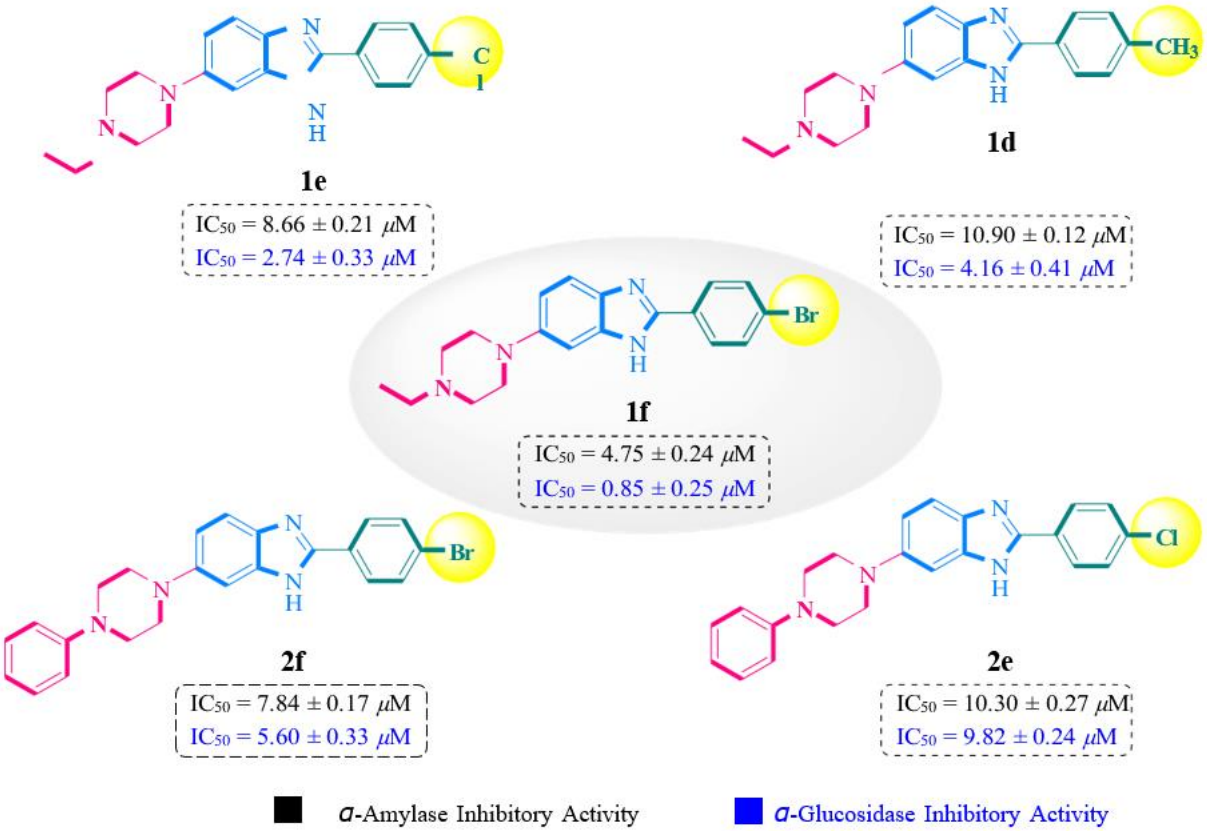

Fig. 2. Structure-activity relationship of most active structures

Results of Kinetic Investigations and in vitro α-Glucosidase Inhibition

The substrate and inhibitor bind to the enzyme's active site in a competitive inhibition manner. As a result, the K_m value rises because the inhibitor now binds to the enzyme's active site rather than the substrate. The affinity of the enzyme for the inhibitor rises with increasing Km values. Table 2 shows that of the competitive inhibitors, compound **1f**, with a K_m value of 1.05 mg/mL, is the inhibitor that the enzyme is most interested in. (Table 2, Figure 3a). In the presence of **2d, 2e,** and **2f,** because of the decreasing of both their Vmax and Km values, which were obtained from the Lineweaver-Burk plots, inhibition type of compounds **2d, 2e,** and **2f** was uncompetitive mode; the inhibitor binds to the only enzyme-substrate complex (Table 2, Figure 3b).

Results of Kinetic Investigations and in vitro α-Amylase İnhibition

Lineweaver-Burk plots were used to determine the kind of enzyme inhibition of the compounds **1f, 2f, 1e, 2e, 1d,** and acarbose, as well as their α-amylase activity using data from enzyme experiments with various quantities of starch in the absence or presence of-

Table 2. Inhibition type of α-glucosidase in the presence of substances 1c, 1d, 1e, 1f, 2d, 2e, 2f, and acarbose with kinetic parameters.

Inhibitors	4–Nitrophenyl α-D-glucopyranoside				
	K_m (mg/mL)	V_{max} (mM/min)	Type of Inhibition	IC_{50} (μM)	R^2
Control	0.31	180.68	-	-	0.989
Acarbose	0.34	180.68	Competitive	14.70	0.993
1c	0.53	180.68	Competitive	10.24	0.990
1d	0.69	180.68	Competitive	4.16	0.989
1e	0.82	180.68	Competitive	2.74	0.991
1f	1.05	180.68	Competitive	0.85	0.993

2d	0.27	145.44	Uncompetitive	11.70	0.997
2e	0.24	120.44	Uncompetitive	9.82	0.992
2f	0.22	108.07	Uncompetitive	5.60	0.995

-each inhibitor (Figures 4a-b and Table 3). Compounds **1d, 1e,** and **1f** raised the K_m value while keeping the V_{max} value constant (270.50 mM/min). The Lineweaver-Burk plots analysis revealed from the data that these structures inhibited in a competitive mode. (Figure 4a). When a competitive substrate inhibits an enzyme, the inhibitor attaches to the enzyme's active site. As a result, the inhibitor bypasses the substrate, which increases the K_m value. The affinity of the enzyme for the inhibitor rises with increasing K_m values. In the presence of **2e** and **2f**, because of the decreasing of both their V_{max} and K_m values, which were obtained from the Lineweaver-Burk plots, inhibition type of compounds **2e** and **2f** was uncompetitive mode, and the inhibitor binds to the only enzyme-substrate complex (Table 3, Figure 4b). According to the results of the kinetic research and amylase enzyme inhibition experiment, compound **1f** with a K_m value of 0.81 mg/mL is the competitive inhibitor the enzyme is most interested in (Table 3, Figures 4a).

In vitro Antioxidant activities

The CUPRAC technique of measuring antioxidant capacity is based on the CUPRAC chromophore's absorbance measurement, Cu(I)–neocuproine (Nc) chelate, generated as a result of the redox interaction between antioxidants and the copper(II) cation, bis(neocuproine) [Cu(II)-Nc], where absorbance is measured at 450 nm, the wavelength at which the lightest may be absorbed.

Due to the formation of the Cu(I)-Nc charge-transfer complex, the color is orange-yellow [35]. The ability of the sample compounds to reduce iron(III) to iron(II) ions was examined using the FRAP assay, and the absorbance of TPTZ(2,4,6-tripyridyl-1,3,5-s-triazine)-Fe^{2+} complex was measured at 593 nm as the activity of the antioxidants increased. According to the absorbance - [$FeSO_4.7H_2O$] calibration graph, the samples' observed absorbance was converted to $FeSO_4.7H_2O$ equivalent antioxidant capacity values, and the resulting µM $FeSO_4.7H_2O$ values are listed in Table 4. In the CUPRAC (CUPRAC value, 27.141 ± 0.022 mM Trolox/mg compound) antioxidant experiment, compound **1d** was discovered to be the most efficient chemical. Compound **2d** was the most effective compound in the FRAP (FRAP value, 9.761 ± 0.019 mM $FeSO_4.7H_2O$/mg compound) method (Table 4). The DPPH technique is based on the observation that the free radical has a purple hue and that in the presence of an antioxidant, the DPPH's purple hue fades. After reduction, the hue shifted from purple to yellow, which may be measured by a decline in absorbance at 517 nm. The findings were represented as SC_{50} (µM), determined from the curves by graphing absorbance values. SC_{50} values show the concentration of the structure (µM) necessary to inhibit 50% of the radicals. Compound **2d** performed the best among the produced compounds due to having the lowest SC_{50} value (19.05±0.21 µM). Following this sequence of action, we may list the compounds whose radical scavenging activity is superior to that of ascorbic acid: **2d > 1d > 2c > 1e > 2b > 2e> 1c > 1f > 1b > 2a > 2f > 2 >** BHT.

The common component of all synthesized compounds, 6-(4-ethyl (phenyl)piperazin-1-yl)-2- (4-substituedphenyl)-1*H*-benzimidazole, undoubtedly contributed to the manifestation of the antioxidant activity. However, a limited SAR connection was identified by examining the various components of the synthesized structure, such as the aryl component. Almost all substances showed increased activity compared to butylated hydroxytoluene. (BHT) (SC_{50} 65.90±0.24 µM). We concluded from the results that the piperazine ring's substitute group is ineffective for antioxidant activities. On the other hand, the substituted group on the *para* position of the phenyl ring is more effective for activity.

Molecular docking studies for α-amylase and α-glucosidase enzymes

The docking investigations with the benzimidazole derivatives revealed a variety of possible interactions with the substrate-binding region of α-amylase (Fig. 5a-c), TRP316, ARG319, ASN431, ASP432, LYS268, and ASN481 are binding site residues that interact with Benzimidazole compounds. Table **5** lists the interaction specifics and docking score. Compound **1f** established significant interaction with the binding site residues of amylase, *i.e.*, Arg195 and Asp300 form hydrogen bond acceptor and donor interaction with docking score of -6.92 (see Fig 5b) proceeded by compound **1e.**

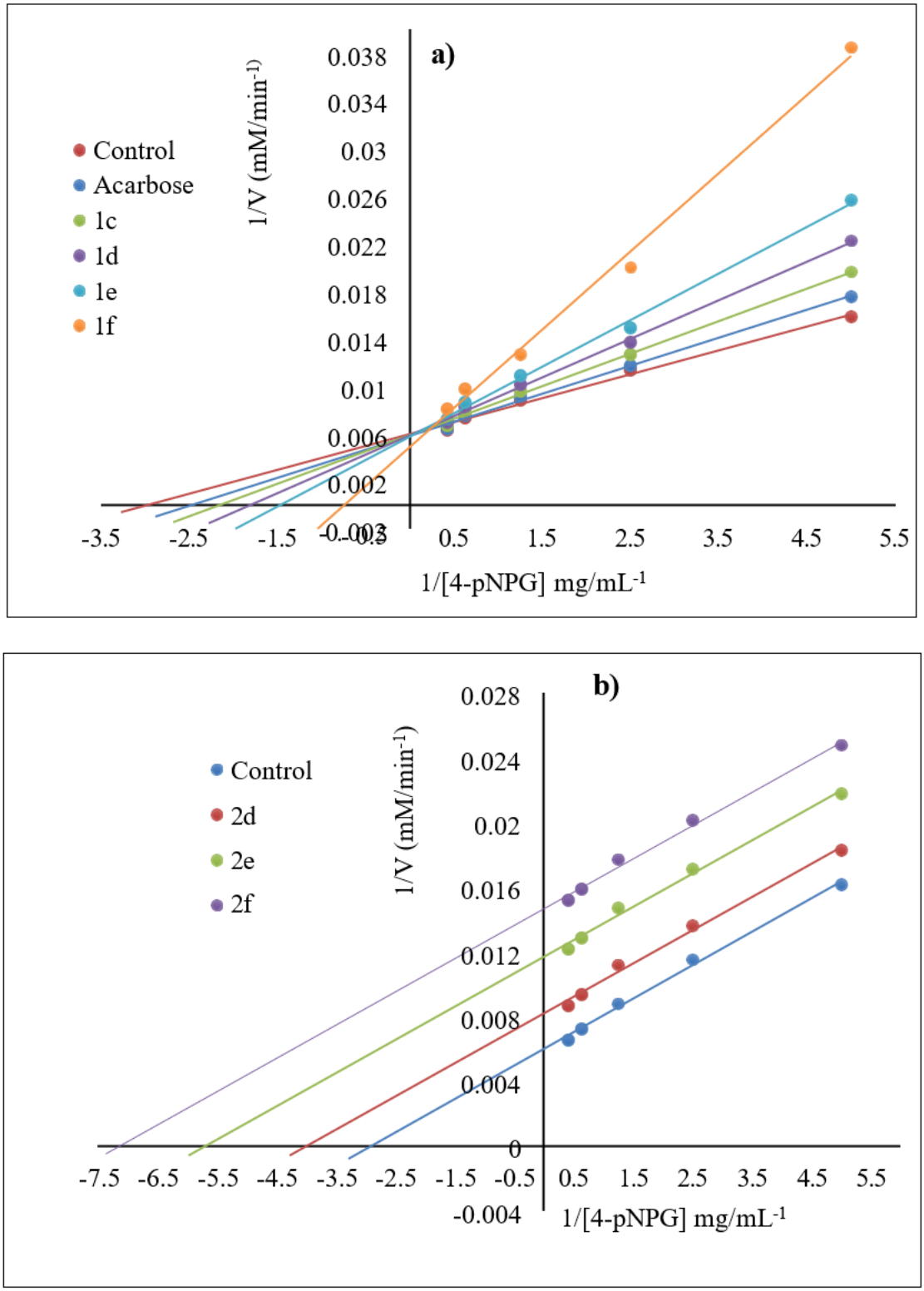

Fig. 3. Types of inhibition and Lineweaver-Burk plots of acarbose, compounds 1c, 1d, 1e and 1f, (a), Control, compounds 2d, 2e and 2f (b) against the α-glucosidase enzyme.

Table 3. Type of α-amylase inhibition of the compounds 1d, 1e, 1f, 2e, 2f, and acarbose with their K_m and V_{max} values.

Inhibitors	Starch				
	K_m (mg/mL)	V_{max} (mM/min)	Type of Inhibition	IC_{50} (µM)	R^2
Control	0.45	270.50	-	-	0.988
Acarbose	0.58	270.50	Competitive	14.70	0.989
1d	0.69	270.50	Competitive	10.90	0.994
1e	0.75	270.50	Competitive	8.66	0.992
1f	0.81	270.50	Competitive	4.75	0.990
2e	0.40	248.45	Uncompetitive	10.30	0.991
2f	0.35	220.06	Uncompetitive	7.84	0.993

which has the docking score of -6.8, forming two hydrogen bond donor, and two hydrogen bond acceptor interactions with ARG267, ASP 433, ARG319, and ASN481 amino acids residues of the *α*-amylase protein (Fig 5a). while in the cause of *α*-glucosidase. The most potent derivative of benzimidazole is compound **1f**, and compound **2f**. Compound **1f** has a docking score of -6.4, forming two hydrogen bond acceptors and two hydrogen bond donor interactions with the key residues of α-glucosidase (Figure 5d). In contrast, the second most potent compound is compound **2f**, which form two hydrogen bond donor interactions with GLU304, PHE α-glucosidase157, and two hydrogen bond acceptor interaction with a docking score of -6.2 (Fig no. 5e). Overall, benzimidazole derivative docking simulations show that electron- withdrawing and denotating substitutions in benzimidazole result in the strong inhibitory actions of amylase. These derivatives were discovered in the substantial interaction with different binding affinities toward both target proteins in contrast to the control acarbose.

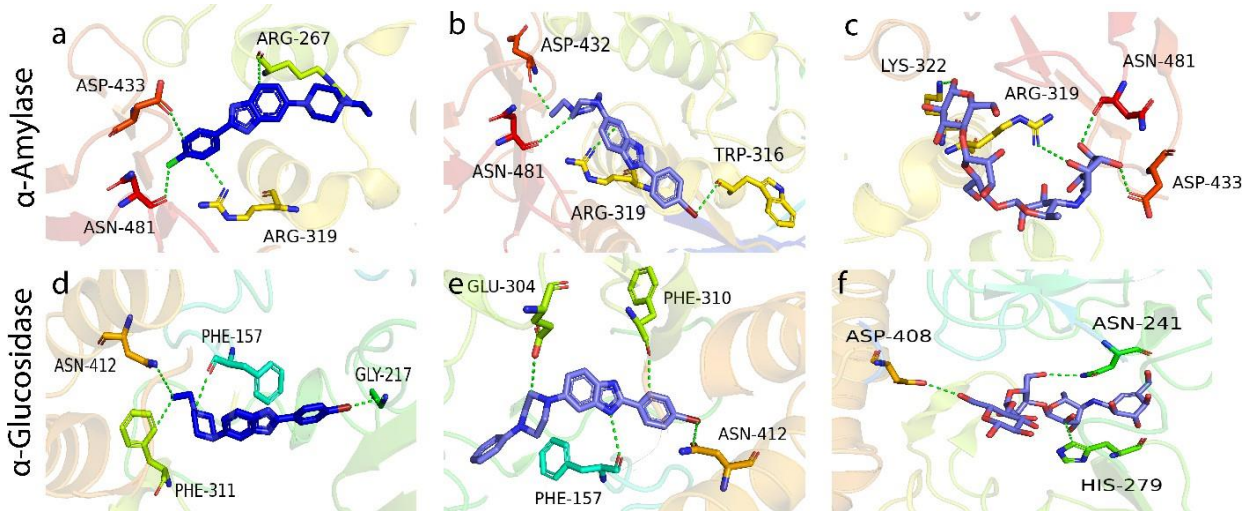

Fig. 5. The docked conformations of the top most active benzimidazole derivatives against α- amylase and αglucosidase.

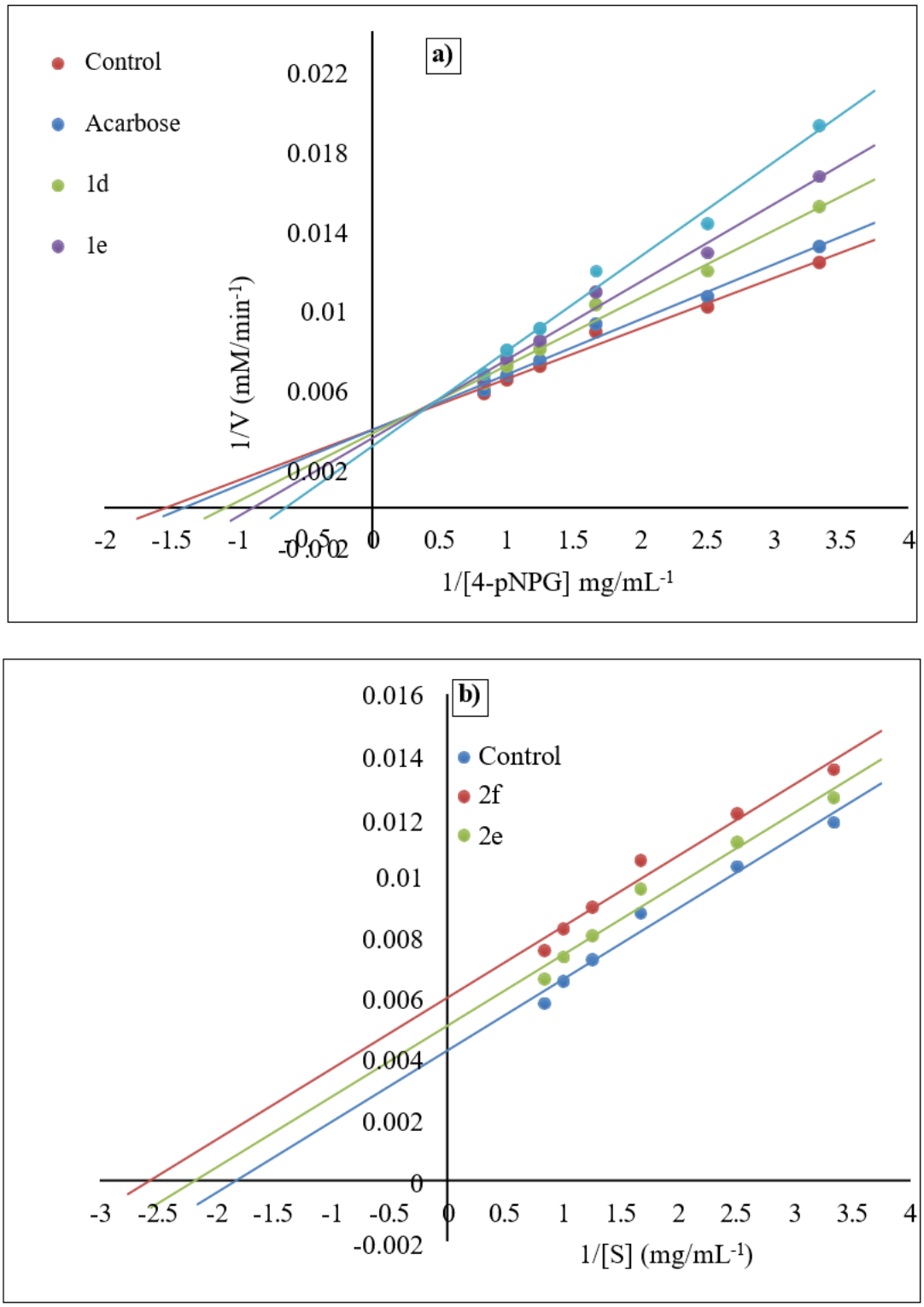

Fig. 4. Types of inhibition and Lineweaver-Burk plots of Control, Acarbose, Compounds 1d, 1e, and 1f (a), and Control, compound 2e and 2f (b) against α-amylase enzyme.

Table 4: Results of tests for antioxidant techniques on all synthesized compounds.	activity using the	CUPRAC, FRAP, and	DPPH
Compound No	CUPRAC[a]	FRAP[b]	DPPH Method[c]
1	8.355 ± 0.022	0.206 ± 0.003	80.55 ± 0.45

1a	21.448 ± 0.013	1.211 ± 0.019	74.90 ± 0.32	
1b	22.422 ± 0.019	2.973 ± 0.038	41.54 ± 0.27	
1c	23.890 ± 0.023	1.757 ± 0.019	37.86 ± 0.66	
1d	27.141 ± 0.022	1.386 ± 0.019	21.45 ± 0.19	
1e	21.987 ± 0.036	1.415 ± 0.020	30.66 ± 0.47	
1f	24.025 ± 0.013	1.415 ± 0.025	38.16 ± 0.24	
2	14.871 ± 0.014	3.886 ± 0.019	61.88 ± 0.56	
2a	17.380 ± 0.005	8.519 ± 0.019	44.75 ± 0.72	
2b	19.860 ± 0.011	8.903 ± 0.013	34.72 ± 0.35	
2c	21.028 ± 0.021	8.553 ± 0.013	25.88 ± 0.79	
2d	25.823 ± 0.028	9.761 ± 0.019	19.05 ± 0.21	
2e	19.639 ± 0.058	6.748 ± 0.040	36.94 ± 0.20	
2f	16.070 ± 0.012	6.578 ± 0.013	55.87 ± 0.34	
BHT	---	---	65.90 ± 0.24	

a**:** mM Trolox/mg compound, b: mM $FeSO_4.7H_20$/mg compound, c: SC_{50} value, µM

Table 5: Represents the docking scores and report of predicted interactions of benzimidazole derivatives toward α-amylase.

Compound	Docking score	Interacting residues	Interaction type	Distance	Energy
1	-4.482	LYS268	H-acceptor	3.21	-1.6
		ARG319	H-acceptor	3.43	-2.5
1a	-4.564	LYS268	H-acceptor	3.65	-4.3
		SER482	H-acceptor	3.34	-1.5
1b	-5.643	ASN430	H-donor	3.23	-0.9
		LYS268	H-acceptor	3.32	-2.1
		LEU320	π-H	3.58	-0.7
1c	-5.734	ASN481	H-donor	3.67	-0.1
		LYS268	H-acceptor	3.75	-0.4
		LYS268	H-acceptor	4.29	-0.1
1d	-6.487	ASN431	H-donor	3.90	-0.1
		ASN431	H-donor	3.73	-0.1
		ARG319	H-acceptor	3.62	-3.1
		LYS268	pi-H	3.72	-2.0
1e	-6.832	ARG267	H-donor	3.45	-0.1
		ASP433	H-donor	3.38	-0.1
		ARG319	H-acceptor	3.97	-0.1
		ASN481	H-acceptor	3.48	-0.2
1f	-6.921	TRP316	H-donor	3.67	-0.1
		ASP432	H-donor	3.30	-0.1
		ASN481	H-donor	3.80	-0.1
		ARG319	H-acceptor	3.81	-0.6
2	-5.684	ASN431	H-donor	2.96	-0.7
		LYS268	H-acceptor	3.12	-3.0
2a	-5.578	ARG267	H-acceptor	3.06	-0.8

		LYS268	H-acceptor	3.94	-0.7
2b	-5.743	ARG319	π-H	3.95	-0.5
		ARG319	π-cation	3.85	-0.3
2c	-5.795	TRP388	H-π	3.75	-0.6
		LYS322	π-cation	3.58	-0.7
2d	-5.832	ASP317	H-acceptor	3.62	-0.5
		ARG319	π-cation	3.55	-0.6
2e	-5.783	LYS322	π-cation	3.36	-1.4
		GLU484	π-H	3.81	-0.5
2f	-5.943	ARG267	H-donor	3.57	-0.1
		ARG319	H-acceptor	4.19	-0.1
		LEU320	π-H	3.89	-0.7
Acarbose	-6.321	ASP433	H-donor	2.84	-3.3
		ASN481	H-donor	2.78	-2.5
		ARG319	H-acceptor	3.13	-1.8
		LYS322	H-acceptor	2.99	-2.9

Table 6: Represents the Docking scores and report of predicted interactions of benzimidazole derivatives toward α-glucosidase.

Compound	Docking score	Interacting residues	Interaction type	Distance	Energy
1	-4.375	HIS279	H-acceptor	3.77	-0.2
		HIS245	H-π	3.96	-0.8
1a	-4.564	PHE157	H-π	3.72	-0.3
		PRO309	π-H	3.95	-0.2
1b	-4.926	ASN412	H-donor	3.19	-0.2
		HIS239	H-π	4.27	-0.4
1c	-5.142	HIS239	H-donor	3.92	-0.4
		HIS245	H-π	3.69	-0.2
1d	-5.439	ASN412	H-donor	-0.3	3.30
		PHE311	π-H	-0.8	4.60
1e	-5.892	GLY 17	H-acceptor	3.14	-0.7
		HIS 245	H-π	3.57	-0.4
		ALA 278	pi-H	3.54	-0.2
1f	-6.421	PHE157	H-donor	3.72	-0.1
		ASN412	H-donor	3.61	-0.1
		PHE311	H-acceptor	3.86	-0.2
		GLY217	H-acceptor	3.39	-0.6
2	-5.612	GLU304	H-donor	3.64	-0.1
		THR215	H-acceptor	3.78	-0.4
2a	-5.312	ARG312	H-acceptor	4.13	-0.1
		HIS245	H-π	3.42	-0.2
2b	-5.536	GLU276	H-donor	3.89	-0.6

		PHE311	H-acceptor	3.60	-0.4
2c	-5.442	GLU276	H-donor	3.65	-0.5
		PHE300	H-π	4.56	-0.9
2d	-5.32	PHE310	H-donor	3.90	-0.2
		PHE157	H-acceptor	4.00	-0.2
2e	-5.853	GLU304	H-donor	3.59	-0.1
		PHE157	H-π	4.21	-0.3
2f	-6.214	GLU304	H-donor	2.99	-0.2
		PHE157	H-donor	3.62	-0.7
		PHE310	H-acceptor	3.90	-0.3
		ASN412	H-acceptor	3.81	-0.2
Acarbose	-6.159	ASP408	H-donor	3.08	-2.1
		ASN241	H-acceptor	3.06	-0.5
		HIS279	H-π	3.72	-0.8

Conclusion

Novel benzimidazole derivatives were developed, synthesized, and evaluated for their capacity to inhibit α-glucosidase and α-amylase and antioxidant activity. These derivatives have a piperazine ring at the C-6 position of the benzimidazole. Rapid "one pot" nitro reductive cyclization was used to quickly develop and efficiently synthesize several new benzimidazoles with the piperazine cycle. The synthesis technique provides low-cost, quick, and effective ways to obtain novel benzimidazole derivatives with good yields of sec-amine derivatives at position C-6. The potential for inhibiting α-glucosidase and α-amylase in the produced benzimidazole compounds was assessed. The inhibitory potential of compounds **1c, 1d, 1e, 1f, 2d, 2e,** and **2f** was significantly greater than that of the common acarbose. The nonplanar ethyl group on the piperazine ring is necessary for the compound to demonstrate biological activity. According to tests of compound activities and SAR, halo groups might increase the binding affinity and provide more potent inhibitory activity. We also defined the antioxidant characteristics of each benzimidazole derivative. The CUPRAC, FRAP, and DPPH techniques revealed that most compounds had potent scavenging activity. All compounds interaction profiles were within the acceptable IC_{50} range, according to *in silico* analyses. The compounds with the highest dock scores were chosen for further molecular analysis against both enzymes. Benzimidazole and piperazine can potentially serve as a source of pharmaceuticals for medicinal purposes.

Declaration of competing interest

The authors declare that they have no known competing financial interests or personal relationships that could have appeared to influence the work reported in this paper.

References

[1] A. M. Pisoschi, A. Pop, The role of antioxidants in the chemistry of oxidative stress: A review, Eur. J. Med. Chem. 97 (2015) 55–74. https://doi.org/10.1016/j.ejmech.2015.04.040.

[2] J. Liu, H. Sun, F. Dong, Q. Xue, G. Wang, S. Qin, Z. Guo, The influence of the cation of quaternized chitosans on antioxidant activity, Carbohydr. Polym. 78 (2009) 439– 443. https://doi.org/10.1016/j.carbpol.2009.04.030.

[3] M. Valko, D. Leibfritz, J. Moncol, M.T. Cronin, M. Mazur, J. Telser, Free radicals and antioxidants in normal physiological functions and human disease, Int. J. Biochem. Cell Biol. 39 (2007) 44–84. https://doi.org/10.1016/j.biocel.2006.07.001.

[4] N. Chattopadhyay, T. Ghosh, S. Sinha, K. Chattopadhyay, P. Karmakar, B. Ray, Polysaccharides from Turbinaria conoides: Structural features and antioxidant capacity, Food Chem. 118 (2010) 823–829. https://doi.org/10.1016/j.foodchem.2009.05.069.

[5] M. Özil, C. Parlak, N. Baltaş, A simple and efficient synthesis of benzimidazoles containing piperazine or morpholine skeleton at C-6 position as glucosidase inhibitors with antioxidant activity, Bioorg. Chem. 76 (2018) 468–477.

[6] A.A. Akande, U. Salar, K.M. Khan, S. Syed, S.A. Aboaba, S. Chigurupati, A. Wadood, M. Riaz, M. Taha, S. Bhatia, Kanwal, S. Shamim, S. Perveen, Substituted Benzimidazole Analogues as Potential α-Amylase Inhibitors and Radical Scavengers, ACS Omega. 6 (2021) 22726–22739. https://doi.org/10.1021/acsomega.1c03056.

[7] Z. Liu, S. Ma, Recent Advances in Synthetic α-Glucosidase Inhibitors, ChemMedChem. 12 (2017) 819–829. https://doi.org/10.1002/cmdc.201700216.

[8] R. Kawamori, N. Tajima, Y. Iwamoto, A. Kashiwagi, K. Shimamoto, K. Kaku, Voglibose

for prevention of type 2 diabetes mellitus: a randomised, double-blind trial in Japanese individuals with impaired glucose tolerance, Lancet. 373 (2009) 1607– 1614. https://doi.org/10.1016/S0140-6736(09)60222-1.

[9] M. Özil, M. Emirik, A. Beldüz, S. Ülker, Molecular docking studies and synthesis of novel bisbenzimidazole derivatives as inhibitors of α-glucosidase, Bioorg. Med. Chem. 24 (2016) 5103–5114. https://doi.org/10.1016/j.bmc.2016.08.024.

[10] M. Özil, M. Emirik, S.Y. Etlik, S. Ülker, B. Kahveci, A simple and efficient synthesis of novel inhibitors of alpha-glucosidase based on benzimidazole skeleton and molecular docking studies, Bioorg. Chem. 68 (2016) 226–235. https://doi.org/10.1016/j.bioorg.2016.08.011.

[11] M. Taha, N.H. Ismail, S. Imran, M.H. Mohamad, A. Wadood, F. Rahim, S.M. Saad, A.U. Rehman, K.M. Khan, Synthesis, α-glucosidase inhibitory, cytotoxicity and docking studies of 2-aryl-7-methylbenzimidazoles, Bioorg. Chem. 65 (2016) 100–109. https://doi.org/10.1016/j.bioorg.2016.02.004.

[12] M.A. Abbas, S. Hameed, M. Farman, J. Kressler, N. Mahmood, Conjugates of Degraded and Oxidized Hydroxyethyl Starch and Sulfonylureas: Synthesis, Characterization, and in Vivo Antidiabetic Activity, Bioconjug. Chem. 26 (2015) 120–127. https://doi.org/10.1021/bc500509a.

[13] F.J. Warren, B. Zhang, G. Waltzer, M.J. Gidley, S. Dhital, The interplay of α-amylase and amyloglucosidase activities on the digestion of starch in in vitro enzymic systems, Carbohydr. Polym. 117 (2015) 192–200.

[14] R. Sindhu, P. Binod, A. Pandey, α-Amylases, in: A. Pandey, S. Negi, C.R.B.T.-C.D. in B. and B. Soccol (Eds.), Curr. Dev. Biotechnol. Bioeng., Elsevier, 2017: pp. 3–24. https://doi.org/10.1016/B978-0-444-63662-1.00001-4.

[15] D. Mijin, B.B. Božić Nedeljković, B. Božić, I. Kovrlija, J. Ladarević, G. Uščumlić, Synthesis, solvatochromism, and biological activity of novel azo dyes bearing 2- pyridone and benzimidazole moieties, Turkish J. Chem. 42 (2018) 896–907. https://doi.org/10.3906/kim-1711-97.

[16] D. Song, S. Ma, Recent Development of Benzimidazole-Containing Antibacterial Agents, ChemMedChem. 11 (2016 646–659. https://doi.org/10.1002/cmdc.201600041.

[17] A. Kanwal, M. Ahmad, S. Aslam, S.A.R. Naqvi, M.J. Saif, Recent Advances in Antiviral Benzimidazole Derivatives: A Mini Review, Pharm. Chem. J. 53 (2019) 179– 187. https://doi.org/10.1007/s11094-019-01976-3.

[18] S. Tahlan, S. Kumar, S. Kakkar, B. Narasimhan, Benzimidazole scaffolds as promising antiproliferative agents: A review, BMC Chem. 13 (2019) 1–16. https://doi.org/10.1186/s13065-019-0579-6.

[19] B. Kahveci, E. Menteşe, M. Özil, S. Ülker, M. Ertürk, An efficient synthesis of benzimidazoles via a microwave technique and evaluation of their biological activities, Monatshefte Fur Chemie. 144 (2013) 993–1001. https://doi.org/10.1007/s00706-012- 0916-0.

[20] E.S. Moghadam, A.M. Al-Sadi, T. Al-Harthy, M.A. Faramarzi, M. Shongwe, M. Amini, R. Abdel-Jalil, Synthesis, bioactivity, and molecular docking of benzimidazole- 2-carbamate derivatives as potent α-glucosidase inhibitors, J. Mol. Struct. 1278 (2023) 134931.

[21] M. Al-Ghorbani, A. Bushra Begum, Z. Zabiulla, S. V. Mamatha, S.A. Khanum, Piperazine and morpholine: Synthetic preview and pharmaceutical applications, Res. J. Pharm. Technol. 8 (2015) 611–628. https://doi.org/10.5958/0974-360X.2015.00100.6.

[22] S. Bhattacharya, P. Chaudhuri, A.K. Jain, A. Paul, Symmetrical bisbenzimidazoles with benzenediyl spacer: The role of the shape of the ligand on the stabilization and structural alterations in telomeric g-quadruplex dna and telomerase inhibition, Bioconjug. Chem. 21 (2010) 1148–1159. https://doi.org/10.1021/bc9003298.

[23] T. De La Fuente, M. Martín-Fontecha, J. Sallander, B. Benhamú, M. Campillo, R.A. Medina, L.P. Pellissier, S. Claeysen, A. Dumuis, L. Pardo, M.L. López-Rodríguez, Benzimidazole derivatives as new serotonin 5-HT6 receptor antagonists. Molecular mechanisms of receptor inactivation, J. Med. Chem. 53 (2010) 1357–1369. https://doi.org/10.1021/jm901672k.

[24] N.T. Chandrika, S.K. Shrestha, H.X. Ngo, S. Garneau-Tsodikova, Synthesis and investigation of novel benzimidazole derivatives as antifungal agents, Bioorg. Med. Chem. 24 (2016) 3680–3686.

[25] H. Nimesh, S. Sur, D. Sinha, P. Yadav, P. Anand, P. Bajaj, J.S. Virdi, V. Tandon, Synthesis and biological evaluation of novel bisbenzimidazoles as Escherichia coli topoisomerase IA inhibitors and potential antibacterial agents, J. Med. Chem. 57 (2014) 5238–5257.

[26] M. Özil, G. Tacal, N. Baltaş, M. Emirik, Synthesis and molecular docking studies of novel triazole derivatives as antioxidant agents, Lett. Org. Chem. 17 (2020) 309–320.

[27] F. Tok, B. Küçükal, N. Baltaş, G. Tatar Yılmaz, B. Koçyiğit-Kaymakçıoğlu, Synthesis of novel thiosemicarbazone derivatives as antidiabetic agent with enzyme kinetic studies and antioxidant activity, Phosphorus. Sulfur. Silicon Relat. Elem. 197 (2022) 1284–1294.

[28] I.F.F. Benzie, J.J. Strain, Ferric reducing (antioxidant) power as a measure of antioxidant capacity: The FRAP assay and its modification for measurement of ascorbic acid (FRASC), Methods Enzymol. 299 (1999) 15–27.

[29] W. Brand-Williams, M.E. Cuvelier, C. Berset, Use of a free radical method to evaluate antioxidant activity, LWT - Food Sci. Technol. 28 (1995) 25–30. https://doi.org/10.1016/S0023-6438(95)80008-5.

[30] S. Hameed, K.M. Khan, U. Salar, M. Özil, N. Baltaş, F. Saleem, U. Qureshi, M. Taha, Z. Ul-Haq, Hydrazinyl thiazole linked indenoquinoxaline hybrids: Potential leads to treat hyperglycemia and oxidative stress; Multistep synthesis, α-amylase, α-glucosidase inhibitory and antioxidant activities, Int. J. Biol. Macromol. 221 (2022) 1294–1312.

[31] N. Baltaş, A-glucosidase and α-amylase inhibition of some ethanolic propolis samples, Uludağ Arıcılık Derg. 21 (2021) 1–7.

[32] H. Lineweaver, D. Burk, The determination of enzyme dissociation constants, J. Am. Chem. Soc. 56 (1934) 658–666.

[33] P.S. Unnikrishnan, K. Suthindhiran, M.A. Jayasri, Alpha-amylase inhibition and antioxidant activity of marine green algae and its possible role in diabetes management, Pharmacogn. Mag. 11 (2015) S511.

[34] F. Saleem, K.M. Khan, N. Ullah, M. Özil, N. Baltaş, S. Hameed, U. Salar, A. Wadood,

A.U. Rehman, M. Kumar, Bioevaluation of synthetic pyridones as dual inhibitors of α-amylase and α-glucosidase enzymes and potential antioxidants, Arch. Pharm. (Weinheim). 356 (2023) 2200400.

[35] R. Apak, S. Gorinstein, V. Böhm, K.M. Schaich, M. Özyürek, K. Güçlü, Methods of measurement and evaluation of natural antioxidant capacity/activity (IUPAC Technical Report), Pure Appl. Chem. 85 (2013) 957–998.

[36] A. Wadood, A. Ajmal, M. Junaid, A.U. Rehman, R. Uddin, S.S. Azam, A.Z. Khan, A. Ali, Machine learning-based virtual screening for STAT3 anticancer drug target, Curr. Pharm. Des. 28 (2022) 3023–3032.

[37] K. Ozadali-Sari, T. Tüylü Küçükkılınç, B. Ayazgok, A. Balkan, O. Unsal-Tan, Novel multi-targeted agents for Alzheimer's disease: Synthesis, biological evaluation, and molecular modeling of novel 2-[4-(4-substitutedpiperazin-1-yl)phenyl]benzimidazoles, Bioorg. Chem. 72 (2017) 208–214. https://doi.org/10.1016/j.bioorg.2017.04.018.

[38] B. Shankar, P. Jalapathi, A. Valeru, A. Kishor Kumar, B. Saikrishna, K.R. Kudle, Synthesis and biological evaluation of new 2-(6-alkyl-pyrazin-2-yl)-1H- benz[d]imidazoles as potent anti-inflammatory and antioxidant agents, Med. Chem. Res. (2017) 1–12. https://doi.org/10.1007/s00044-017-1897-7.

[39] H. Sharghi, M. Aberi, P. Shiri, Highly reusable support-free copper(II) complex of para -hydroxy-substituted salen: Novel, efficient and versatile catalyst for C─N bond forming reactions, Appl. Organomet. Chem. 31 (2017) e3761. https://doi.org/10.1002/aoc.3761.

[40] R.A. Denny, A.C. Flick, J. Coe, J. Langille, A. Basak, S. Liu, I. Stock, P. Sahasrabudhe, P. Bonin, D.A. Hay, P.E. Brennan, M. Pletcher, L.H. Jones, E.L.P. Chekler, Structure-Based Design of Highly Selective Inhibitors of the CREB Binding Protein Bromodomain, J. Med. Chem. 60 (2017) 5349–5363. https://doi.org/10.1021/acs.jmedchem.6b01839.

[41] M.E. Van Dort, H. Hong, H. Wang, C.A. Nino, R.L. Lombardi, A.E. Blanks, S. Galb. n, B.D. Ross, Discovery of Bifunctional Oncogenic Target Inhibitors against Allosteric Mitogen-Activated Protein Kinase (MEK1) and Phosphatidylinositol 3- Kinase (PI3K), J. Med. Chem. 59 (2016) 2512–2522. https://doi.org/10.1021/acs.jmedchem.5b01655.

[42] R.S. Kankate, P.S. Gide, D.P. Belsare, Design, synthesis and antifungal evaluation of novel benzimidazole tertiary amine type of fluconazole analogues, Arab. J. Chem. (2015). https://doi.org/10.1016/j.arabjc.2015.02.002.

[43] N.R. Thimmegowda, S. Nanjunda Swamy, C.S. Ananda Kumar, Y.C. Sunil Kumar, S. Chandrappa, G.W. Yip, K.S. Rangappa, Synthesis, characterization and evaluation of benzimidazole derivative and its precursors as inhibitors of MDA-MB-231 human breast cancer cell proliferation, Bioorganic Med. Chem. Lett. 18 (2008) 432–435. https://doi.org/10.1016/j.bmcl.2007.08.078.

[44] D. Yang, D. Fokas, J. Li, L. Yu, C.M. Baldino, A versatile method for the synthesis of benzimidazoles from o-nitroanilines and aldehydes in one step via a reductive cyclization, Synthesis (Stuttg). (2005) 47–56. https://doi.org/10.1055/s-2004-834926.

[45] H. Naeimi, N. Alishahi, An efficient and one-pot reductive cyclization for synthesis of 2-substituted benzimidazoles from o-nitroaniline under microwave conditions, J. Ind. Eng. Chem. 20 (2014) 2543–2547. https://doi.org/10.1016/j.jiec.2013.10.038.

[46] Ahmad, T., Muheyuddeen, G., Alam, M., & Aziz, I. (2024). *Unveiling the Promising Potential of Spermidine (Polyamines): Recent Advancements and Emerging Perspectives*. *27*(3).

[47] Muheyuddeen, G., Husain Rayini, S., Yadav, P., & Kumar Gupta, S. (2023). In vivo Analgesics and in vitro Antioxidants Activity of Newly Synthesized Mannich Bases of Lawsone. *Asian Journal of Pharmaceutical Research*, *13*(1), 11–17. https://doi.org/10.52711/2231-5691.2023.00002

[48] Muheyuddeen, G., Rav Divya, S., Verma, S., Kumar Gautam, S., & Kumar Gupta, S. (2023). Lawsonia inermis Linnaeus: Pharmacological Peculiarity and Modern Progression. *Research Journal of Pharmacognosy and Phytochemistry*, *15*(01), 63–76. https://doi.org/10.52711/0975-

4385.2023.00010

[49] Muheyuddeen, G., Singh, S., Nishchaya, K., & Divya, S. R. (2022). *Synthesis and pharmacological evaluation of aniline derivatives as a potent analgesic and antioxidant agent*. *20*(11), 7040–7055. https://doi.org/10.14704/NQ.2022.20.11.NQ66701